HHS Public Access

Author manuscript

Cell Rep. Author manuscript; available in PMC 2022 April 13.

Published in final edited form as:

Cell Rep. 2022 March 29; 38(13): 110576. doi:10.1016/j.celrep.2022.110576.

Developmental coupling of cerebral blood flow and fMRI fluctuations in youth

Erica B. Baller[1,2], **Alessandra M. Valcarcel**[3,9], **Azeez Adebimpe**[1,2], **Aaron Alexander-Bloch**[2], **Zaixu Cui**[1,2], **Ruben C. Gur**[2,4,6], **Raquel E. Gur**[2,4,6], **Bart L. Larsen**[1,2], **Kristin A. Linn**[3], **Carly M. O'Donnell**[3], **Adam R. Pines**[1,2], **Armin Raznahan**[5], **David.R. Roalf**[2], **Valerie J. Sydnor**[1,2], **Tinashe M. Tapera**[1,2], **M. Dylan Tisdall**[6], **Simon Vandekar**[7], **Cedric H. Xia**[1,2], **John A. Detre**[4], **Russell T. Shinohara**[3,8,10], **Theodore D. Satterthwaite**[1,2,8,10,11,*]

[1]Penn Lifespan Informatics and Neuroimaging Center (PennLINC), University of Pennsylvania, Richards Building, 5th Floor, Suite 5A, 3700 Hamilton Walk, Philadelphia, PA 19104, USA

[2]Department of Psychiatry, University of Pennsylvania, Philadelphia, PA 19104, USA

[3]Penn Statistics in Imaging and Visualization Center (PennSIVE), Department of Biostatistics, Epidemiology and Informatics, University of Pennsylvania, Philadelphia, PA 19104, USA

[4]Department of Neurology, University of Pennsylvania, Philadelphia, PA 19104, USA

[5]National Institute of Mental Health, NIH, IRP, Bethesda, MD 20892, USA

[6]Department of Radiology, University of Pennsylvania, Philadelphia, PA 19104, USA

[7]Department of Biostatistics, Vanderbilt University, Nashville, TN 37203, USA

[8]Center for Biomedical Image Computing and Analytics (CBICA), University of Pennsylvania, Philadelphia, PA 19104, USA

[9]Present address: Genentech, Inc., 1 DNA Way, South San Francisco, CA 94080, USA

[10]These authors contributed equally

[11]Lead contact

SUMMARY

*Correspondence: satterth@pennmedicine.upenn.edu.

AUTHOR CONTRIBUTIONS

Conceptualization, E.B.B., R.T.S., and T.D.S.; methodology, E.B.B., R.T.S., T.D.S., J.A.D., K.A.L., A.M.V., A.A.-B., and S.V.; investigation, E.B.B., A.M.V., A.A., and K.A.L.; validation, A.A.; data curation, C.M.O'D., D.R.R., and T.M.T.; formal analysis, E.B.B.; writing – original draft, E.B.B.; writing – review & editing, E.B.B., A.M.V., A.A., A.A.-B., Z.C., R.C.G., R.E.G., A.L.L., K.A.L., C.M.O'D., A.R.P., A.R., D.R.R., V.J.S., T.M.T., M.D.T., S.V., C.H.X., J.A.D., R.T.S., and T.D.S.; funding acquisition, T.D.S., R.T.S., R.E.G., R.C.G., and E.B.B.; resources, T.D.S. and R.T.S.; visualization, A.R.P., C.H.X., and B.L.L.; supervision, R.T.S. and T.D.S.

DECLARATION OF INTERESTS

The authors have no competing interests.

INCLUSION AND DIVERSITY

We worked to ensure gender balance in the recruitment of human subjects. One or more of the authors of this paper self-identifies as a member of the LGBTQ+ community. One or more of the authors of this paper self-identifies as an underrepresented ethnic minority in science. While citing references scientifically relevant for this work, we also actively worked to promote gender balance in our reference list.

The functions of the human brain are metabolically expensive and reliant on coupling between cerebral blood flow (CBF) and neural activity, yet how this coupling evolves over development remains unexplored. Here, we examine the relationship between CBF, measured by arterial spin labeling, and the amplitude of low-frequency fluctuations (ALFF) from resting-state magnetic resonance imaging across a sample of 831 children (478 females, aged 8–22 years) from the Philadelphia Neurodevelopmental Cohort. We first use locally weighted regressions on the cortical surface to quantify CBF-ALFF coupling. We relate coupling to age, sex, and executive functioning with generalized additive models and assess network enrichment via spin testing. We demonstrate regionally specific changes in coupling over age and show that variations in coupling are related to biological sex and executive function. Our results highlight the importance of CBF-ALFF coupling throughout development; we discuss its potential as a future target for the study of neuropsychiatric diseases.

Graphical abstract

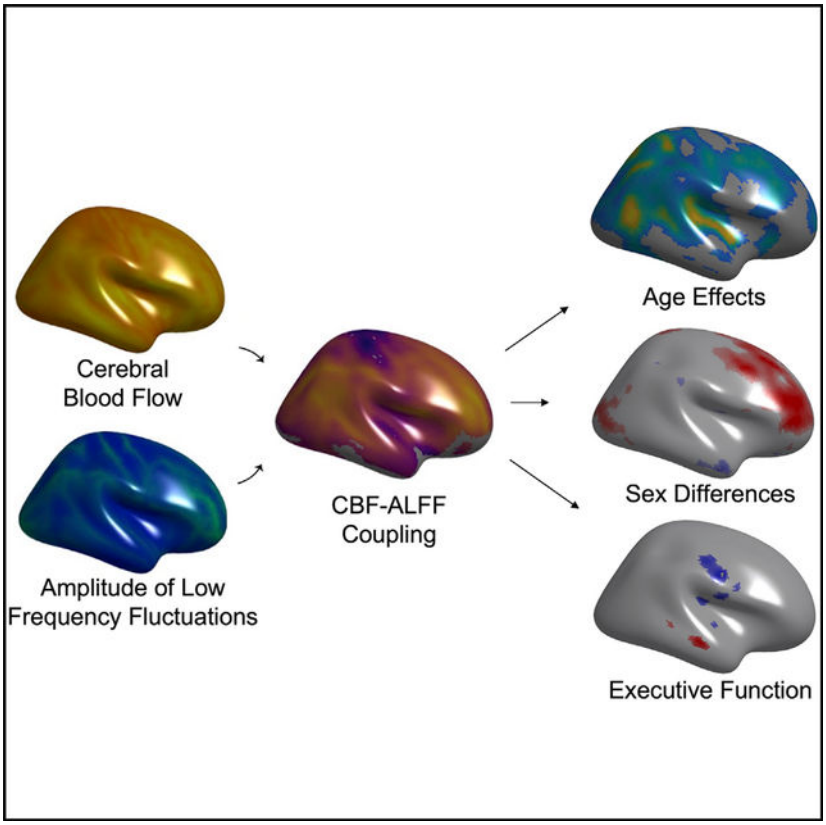

In brief

The functions of the human brain are metabolically expensive and reliant on neurovascular coupling between cerebral blood flow and neural activity, yet how this coupling evolves over development remains unresolved. Here, Baller et al. show that neurovascular coupling evolves over adolescence, differs by sex, and relates to executive function.

INTRODUCTION

The functions of the human brain are metabolically expensive: despite only weighing 1.5 kg on average, the brain comprises a disproportionate one-fifth of bodily energetic requirements (Attwell and Laughlin, 2001; Kety, 1957; Sokoloff, 1996). To meet such large metabolic demands, the brain receives 20% of cardiac output (Williams and Leggett, 1989; Xing et al., 2017). In healthy individuals, the relationship between brain activity and cerebral blood flow (CBF), or neurovascular coupling, is tightly linked at the local level (Armstead, 2016; Kim and Filosa, 2012; Phillips et al., 2016). Under normal circumstances, metabolites produced during neuronal activity cause vasodilation in the microvasculature, and thus a localized increase in blood flow, to increase glucose and oxygen delivery to active cells (Armstead, 2016; Girouard and Iadecola, 2006a; Kim and Filosa, 2012; Phillips et al., 2016). By coupling metabolic demand (neural activity) and supply (blood flow), the neurovascular unit maintains appropriate energy balance (Girouard and Iadecola, 2006a).

To measure neurovascular coupling *in vivo*, proxies for both localized blood flow and regional brain activity are required. Neurovascular coupling has thus been frequently characterized by relating two neuroimaging-derived measures: CBF and the amplitude of low-frequency fluctuations in resting-state blood-oxygen-level-dependent (BOLD) fMRI (ALFF; 10–12). Mean CBF can be imaged reliably and without radiation exposure using arterial spin-labeled (ASL) MRI (Detre and Alsop, 1999; Li et al., 2012; Zheng et al., 2019) and is linked to regional metabolic demands and steady-state neural activity. Low amplitude fluctuations in BOLD signal as measured by ALFF represent fluctuations in brain activity that underlie intrinsic functional connectivity (Cordes et al., 2001). Thus, although BOLD signal changes include contributions from CBF, ALFF is thought to provide a non-invasive proxy of dynamic neuronal activity (Biswal et al., 1995; Zou et al., 2008).

Neurovascular coupling as measured by CBF-ALFF evolves during aging, with younger adults displaying higher coupling than healthy older adults (Garrett et al., 2017; Girouard and Iadecola, 2006a). Young adults are known to have increased BOLD signal variability, which is thought to support a flexible, efficient system and may contribute to higher coupling (Garrett et al., 2017; Nomi et al., 2017). This high degree of efficiency corresponds to the maturation of white matter microstructure at the conclusion of large-scale brain myelination (Giedd et al., 1999; Miller et al., 2012; Sydnor et al., 2021). As normal aging progresses, blood vessels harden and show a decreased vascular response to neural activity, leading to suboptimal coupling and mild neurocognitive decline (Garrett et al., 2017; Lourenço et al., 2018; Nomi et al., 2017; Raz et al., 2007; Sorond et al., 2008), although homeostasis is still generally maintained (Girouard and Iadecola, 2006a; Toth et al., 2017). In contrast, severe decreases in the typically strong coupling between CBF and ALFF have been reported in degenerative and metabolic diseases (Girouard and Iadecola, 2006b; Hu et al., 2019; Jin et al., 2020). Notably, these diseases are associated with significant cognitive impairments, further highlighting the importance of the integrity of this coupling relationship.

Despite this growing literature, notable gaps remain. First, previous studies have focused on neurovascular coupling only in healthy and medically ill adults (Girouard and Iadecola,

2006b; Hu et al., 2019; Jin et al., 2020; Liang et al., 2013; Presa et al., 2020). To our knowledge, no prior research has explored how the relationship between blood flow and brain function evolves during childhood, adolescence, and young adulthood. Thus, it is presently unclear how the balance between metabolic demand and supply changes as neurodevelopment unfolds. Second, previous studies have examined the relationship between CBF and ALFF primarily at the whole-brain level, yielding a global measure of coupling (Gur et al., 2021). While informative, such an approach obscures potentially important regional variation in the coupling between CBF and ALFF.

Here, we sought to define the local relationship between CBF and ALFF on a regional basis, and to determine how a proxy of neurovascular coupling evolves over development. To do this, we capitalized on data from the Philadelphia Neurodevelopmental Cohort: a large-scale, community-based study of brain development that included both ASL MRI and fMRI (Satterthwaite et al., 2014a, 2016). We characterized the CBF-ALFF relationship using recently developed tools for inter-modal coupling analysis that allowed us to describe the local relationships between these two imaging modalities (Vandekar et al., 2015, 2016). As described below, we demonstrated that CBF-ALFF coupling undergoes substantial evolution in youth, differs by sex, and relates to individual differences in executive function.

RESULTS

We investigated how a non-invasive proxy of neurovascular coupling develops in youth, relates to biological sex, and is associated with executive function. To do this, we studied 831 youth who completed both ASL and resting-state fMRI scans as part of the PNC (Figure 1). For each subject, local cortical CBF-ALFF relationships were evaluated using a locally weighted regression at each location (vertex). This was repeated at all vertices for each participant, generating one cortical CBF-ALFF coupling map per participant (Figure 2). To minimize the possibility that our findings were driven by relationships in areas with poor signal-to-noise ratios (SNRs), we removed vertices with SNR < 50 from our analyses. Using spin-based permutation testing (Alexander-Bloch et al., 2018), we confirmed that there was no correlation between the mean CBF-ALFF coupling map and fMRI SNR ($r = 0.17$, spin-based permutation testing $p > 0.1$).

Statistical analyses of age, sex, and executive function used these participant-level CBF-ALFF coupling maps. To flexibly account for both linear and nonlinear developmental effects within a rigorous statistical framework, we modeled age as a spline using generalized additive models (GAMs) (Wood et al., 2015). Multiple comparisons were accounted for using the false discovery rate ($Q < 0.05$).

CBF and ALFF are significantly coupled

We began by evaluating mean CBF-ALFF coupling patterns across the cortex. Replicating previous findings in adults, we observed robust CBF-ALFF coupling across the cortical mantle (Figure 3A). Coupling was strongest in association cortices, including frontal, parietal, and temporal cortex ($p_{fdr} < 0.05$). To test whether coupling patterns were enriched in previously defined functional networks (Thomas Yeo et al., 2011), we used spin-based permutation testing (Alexander-Bloch et al., 2018). Spin-based enrichment testing compared

the proportion of significant vertices within a brain network in real data to that in a conservative, spin-based null distribution that preserved the spatial covariance structure of the data. Network enrichment analysis revealed enrichment of CBF-ALFF coupling in the frontoparietal network ($p = 0.005$; Figure 3B).

CBF-ALFF coupling declines with adolescent development

Having found robust CBF-ALFF coupling in youth, we next evaluated how CBF-ALFF coupling evolved over development. We found that that mean cortical coupling decreased across development ($F_{3,828} = 60.0$, $p < 0.0001$; Figure 4A). The rate of change was not constant, however. Analysis of the derivative of the spline revealed that coupling significantly decreased between the ages of 11.6 and 20.5 years, with a peak decline observed during mid-adolescence at age 16 years. Widespread declines in CBF-ALFF coupling were found across much of the cortex, with peak effects present in the posterior temporal cortex ($p_{fdr} < 0.05$, r^2 range = 0.01–0.1; Figure 4B). Network enrichment analysis revealed that age-related declines in coupling were most prominent in the dorsal attention network ($p = 0.027$; Figure 4C).

CBF-ALFF coupling is higher in females within the frontoparietal network

Sex differences in brain function have been consistently documented in unimodal imaging studies of adolescents (Chung et al., 2019; Reding et al., 2021; Satterthwaite et al., 2014b). Having established significant declines in CBF-ALFF coupling with age, we next evaluated sex differences in CBF-ALFF coupling. We found that females had stronger coupling than males in bilateral dorsolateral prefrontal cortex, medial frontal cortex, anterior cingulate cortex, and precuneus. In contrast, females had lower coupling in the cuneus and lateral temporal cortex ($p_{fdr} < 0.05$, r^2 range = 0.02–0.04; Figure 5A). Spin testing revealed that sex differences in coupling were enriched within the frontoparietal network ($p = 0.032$; Figure 5B).

Age-by-sex interactions were not significant.

CBF-ALFF coupling is associated with executive function

Executive function is a broad domain of cognition that includes working memory, cognitive control, task switching, and response inhibition (Miyake et al., 2000). Executive function undergoes protracted development in adolescence and young adulthood; executive dysfunction is associated with both poor academic outcomes and diverse neuropsychiatric illness (Satterthwaite et al., 2013; Shanmugan et al., 2016; Wade et al., 2020). As a final step, we evaluated the relationship between CBF-ALFF coupling and executive function. We found that better executive function was related to higher coupling in default mode regions, including the posterior cingulate cortex, medial prefrontal cortex, and left temporoparietal junction. Furthermore, lower executive function was also related to more coupling in bilateral motor cortex and primary auditory cortex, including Heschl's gyrus ($p_{fdr} < 0.05$, r^2 range = 0.02–0.03; Figure 6A). Spin testing revealed enrichment of significant associations with executive function within the somatomotor network ($p = 0.040$; Figure 6B).

DISCUSSION

Using a recently developed statistical method for assessing inter-modal coupling and a large sample of youth, we demonstrated significant CBF-ALFF coupling across the cortex.

Furthermore, we identified age-related declines in coupling that were broadly distributed across the cortex and were enriched in the dorsal attention network. In addition, we found that sex differences in CBF-ALFF coupling were enriched within the frontoparietal network. Finally, we highlighted the relevance of CBF-ALFF coupling for cognition by showing significant associations between CBF-ALFF with executive function. Taken together, these results extend prior results in adults and demonstrate that CBF-ALFF coupling undergoes a process of developmental calibration that is relevant for cognition.

Neurovascular coupling is thought to reflect the interrelationship between nutrient demand and supply, whereby neuronal activity influences local changes in blood flow (Armstead, 2016; Kim and Filosa, 2012; Presa et al., 2020; Silverman and Petersen, 2022). At the cellular level, researchers have demonstrated a close relationship between blood flow and neural function that is usually facilitated by communicating astrocytes, where ionic gradients and metabolic biproducts from firing neurons lead to local vasodilation of cerebral arterioles (Blanco et al., 2008; Takano et al., 2006). As such, high coupling could be conceptualized as an optimized, high-fidelity system, where local activity of the vascular unit is influenced by neuronal function (Mulligan and MacVicar, 2004). Previous work has suggested that CBF-ALFF coupling may be understood as a proxy of neurovascular coupling, allowing a non-invasive window into this process (Girouard and Iadecola, 2006b; Hu et al., 2019; Jin et al., 2020).

Highly metabolically active regions, particularly in association networks that coordinate brain activity across distributed brain regions, tend to have increased CBF as well as ALFF (Passow et al., 2015; Zou et al., 2008). Here, we showed that CBF-ALFF coupling is enriched in the frontoparietal network (FPN). Transmodal association cortices that subserve the FPN have larger pyramidal neurons with greater spine and synapse density than pyramidal neurons expressed in other parts of the brain (Beul and Hilgetag, 2019; Elston et al., 2009; Jacobs et al., 2001). Similarly, these association networks are the most spatially distributed, with more long-distance corticocortical connections (Bassett et al., 2008; Bazinet et al., 2020; Jung et al., 2017; Sepulcre et al., 2010). These neuroanatomical features produce greater metabolic activity and thus may demand a tighter link between activity and blood flow (Liang et al., 2013; Shokri-Kojori et al., 2019).

Although coupling remained tight across development and into young adulthood, CBF-ALFF coupling decreased across much of the cortex, with the greatest rate of change during mid-adolescence. These findings coincide with many previously described microscale structural developmental brain changes (Ball et al., 2019; Baum et al., 2020; Giedd et al., 1999; Tamnes et al., 2017; Vázquez-Rodríguez et al., 2019). During the second decade of life, synapses and dendritic spines are pruned to facilitate more efficient between-neuron communication (Arain et al., 2013; Bercury and Macklin, 2015; Paquola et al., 2019; Yurgelun-Todd, 2007). To support these structural changes, perineuronal nets surround the

cell bodies and dendrites and control ion flow and conduction (Fawcett et al., 2019). One possibility is that these structural and ionic adaptations reduce the metabolic demands of the neurons, which has been previously demonstrated in perfusion studies (Liu et al., 2018; Satterthwaite et al., 2014b). These refined local neural circuits may allow for fluctuations in neural activity to be supported by a lower level of metabolic substrate delivered by blood flow.

In addition to cytoarchitectural changes, white matter development at the macroscale may also influence local neurovascular coupling relationships. Changes in neurovascular coupling that occur across development parallel development of cerebral white matter, which reflects enhanced myelination by oligodendrocytes (Baum et al., 2020; Giedd et al., 1999; Miller et al., 2012; Paquola et al., 2019). Oligodendrocytes also deliver metabolic substrates to neurons, providing more metabolic support along the axon rather than just at the cell body (Stadelmann et al., 2019; Suminaite et al., 2019). Importantly, axons supporting long-range cortical connectivity in association cortex myelinate later during development (Miller et al., 2012; Váša et al., 2018). It is possible that at the termination of adolescent developmental myelination, sending the same neural impulse may place lower metabolic demand on the neuron cell body. As a result, engaging in the same low-frequency firing patterns would require less blood flow and thus lead to decreased neurovascular coupling.

In the context of the lifespan, early adulthood may be a time period where optimal neurovascular homeostasis is reached, with the dynamic relationship between blood flow and neural activity supporting maximum metabolic and cognitive efficiency (Girouard and Iadecola, 2006b). As aging progresses, cortical thickness decreases are a product of tissue loss rather than network refinement (Zheng et al., 2019). In addition, the brain undergoes stress, which often manifests in structural, vascular, and metabolic diseases (Girouard and Iadecola, 2006b; Hu et al., 2019; Jin et al., 2020; Presa et al., 2020). The summative effects of these insults may overwhelm neurovascular homeostasis and explain why aging, dementia, strokes, and metabolic diseases are associated with a steep, later-life decrease in neurovascular coupling as well as cognitive decline (Garrett et al., 2017; Girouard and Iadecola, 2006b).

Sex differences in coupling followed a different pattern than age-related changes. Females showed significantly higher coupling in the FPN, which is essential for cognitive control (Dosenbach et al., 2007). Interestingly, previous literature has demonstrated that prominent sex differences in perfusion also emerge during the same developmental window, when girls experience an increase in circulating ovarian estrogens (Janfaza et al., 2006; Kaczkurkin et al., 2016; Satterthwaite et al., 2014b). The neuroactive steroid 17B estradiol, the primary estrogen secreted from the ovary, functions as a potent neurovasodilator by enhancing the production of nitric oxide (Krause et al., 2011). Neurophysiologic studies have consistently demonstrated larger cerebral blood vessel diameter per unit blood pressure in females compared with males (Gündling et al., 1985; Liu et al., 2012). Estrogen is also known to selectively increase blood flow in executive areas in adults (Berman et al., 1997) and emerging evidence has established a link between higher estradiol levels and greater dorsolateral prefrontal cortex activity during emotion regulation in adolescents (Chung et

al., 2019). It is possible that hormone-mediated mechanisms contribute to observed sex differences in coupling within the FPN.

Understanding sex differences in frontoparietal neurobiology that emerge in adolescence is critically important given that mood and anxiety disorders, which are twice as prevalent in girls than boys, also emerge during the same developmental window (Dhamala et al., 2019; Seney and Sibille, 2014). The adult literature consistently reports altered FPN functioning in depression and anxiety (Kaiser et al., 2015; Sylvester et al., 2012), and these differences can also be identified in development. Previous fMRI research has linked variations in frontoparietal network function with phenotypic heterogeneity in youth depression (Baller et al., 2020) and anxiety disorders (Fitzgerald et al., 2013). As a next step, it will be important to study whether frontoparietal coupling could be used as a biomarker for sex differences in psychopathology.

The relevance of CBF-ALFF coupling to cognitive function is supported by our results, which detail a significant age-independent relationship between CBF-ALFF coupling and executive function. Specifically, better executive function was associated with lower coupling in the somatomotor network and higher coupling in regions within the DMN, including the posterior cingulate cortex and medial prefrontal cortex. Our findings align with previous unimodal neuroimaging literature on cognition in youth, where executive functioning has been related to both lower-order sensorimotor networks as well as higher-order association networks (Gilbert et al., 2019; Satterthwaite et al., 2013). Some previous studies have also suggested a dissociation between how executive functioning relates to neuroimaging measures of sensorimotor and association cortices (Schulte et al., 2020). Our findings may further indicate that the development of executive function in youth relies on a balance between decreased coupling in lower-order networks, and temporarily increased coupling in higher-order association networks.

Specifically, the negative correlation in the somatomotor cortex may indicate a refined circuit, where local fluctuations in neural activity can be supported by lower cerebral blood flow. This aligns with previous studies where a strong link exists between motor and executive functioning throughout youth (Livesey et al., 2006; Stöckel and Hughes, 2016; van der Fels et al., 2015), but that no such relationship is present in young adults (Spedden et al., 2017; Stuhr et al., 2020). Higher correlation of executive functioning with neurovascular coupling in regions of the DMN could suggest that this system is undergoing developmental tuning and is therefore not at maximal metabolic efficiency. Although we cannot address it due to the age range of our sample, we speculate that the relationship between coupling and executive functioning may change and become negative in the association cortex after age 20 years, as the brain completes maturation.

Limitations of the study

There are several limitations to our study which should be noted. Previous authors have understood CBF-ALFF coupling as a representation of neurovascular coupling, which has framed our understanding of this measure (Hu et al., 2019; Jin et al., 2020; Zheng et al., 2019). However, we are not able to measure neurovascular coupling directly and had to rely on proxy measures to characterize neurovascular coupling *in vivo*. Typically, positron

emission tomography has generally been the gold standard for measuring blood flow, whereas we use ASL to quantify CBF. However, previous studies have demonstrated good correlation between PET and ASL (Detre and Alsop, 1999). Given the potential risks of radiologic exposure to children with PET scanning, CBF as measured by ASL is a much safer method for use in large-scale studies of youth (Proisy et al., 2016; Wang et al., 2003; Ye et al., 2000). In addition, ALFF is derived from the BOLD signal, which inherently has a vascular component (Tong et al., 2016). However, numerous past studies have suggested that ALFF signals reflect neural activity and that BOLD and CBF fMRI measures capture unique variance (Biswal et al., 1995; Bu et al., 2019; Cordes et al., 2001; Qiu et al., 2017; Yu-Feng et al., 2007). Of note, the spatial resolution of the ASL scan used to measure CBF was less than that of the fMRI scan used to measure ALFF. While all analyses were conducted at the cortical surface in template space, the low resolution of the ASL acquisition may have limited our ability to discern fine-grained changes in coupling. Finally, we evaluated a cross-sectional sample that prevents us from estimating within-individual change; future studies in longitudinal samples will be important.

The limitations notwithstanding, we provide evidence for the developmental evolution of CBF-ALFF coupling in youth, as well as distinct associations with sex and executive function. Our findings suggest numerous avenues for future study. Longitudinal assessments that allow for the measurement of within-subject change in coupling across the lifespan may help us better understand normal physiologic brain development and aging at a personalized level. Studies that combine direct measures of neural activity, such as electroencephalography or magneto-encephalography, with CBF may provide further insights into neurovascular coupling dynamics. In addition, transdiagnostic deficits in executive functioning are commonly observed across psychiatric illnesses (Satterthwaite et al., 2013; Shanmugan et al., 2016; Wade et al., 2020). Given that deficits in executive functioning were associated with altered CBF-ALFF coupling, future studies could yield important insights into whether regional differences in CBF-ALFF coupling are linked to the onset and development of psychopathology. Eventually, characterizing neurovascular coupling in youth at risk may aid in the development of targeted pharmacologic and neurotherapeutic treatments.

STAR★METHODS

RESOURCE AVAILABILITY

Lead contact—Any additional information or inquiries regarding code availability or resources should be directed to Theodore Satterthwaite (sattertt@pennmedicine.upenn.edu).

Materials availability—This study did not generate new unique reagents.

Data and code availability—This paper analyzes existing, publicly available data from the Philadelphia Neurodevelopmental Cohort. https://www.ncbi.nlm.nih.gov/projects/gap/cgi-bin/study.cgi?study_id=phs000607.v3.p2.

To request access, an authorization request can be completed via https://dbgap.ncbi.nlm.nih.gov/aa/wga.cgi?login=&page=login.

All original code has been deposited at https://pennlinc.github.io/IntermodalCoupling/ and is publicly available as of the date of publication. DOIs are listed in the Key Resources table.

Any additional information required to reanalyze the data reported in this paper is available from the lead contact upon request.

EXPERIMENTAL MODEL AND SUBJECT DETAILS

Participants were drawn from the Philadelphia Neurodevelopmental Cohort (PNC). As previously described, a total of 9,498 participants aged 8–22 years received cognitive assessment and clinical phenotyping, and a subset of 1,601 youths also completed neuroimaging as part of the PNC (Calkins et al., 2015; Satterthwaite et al., 2014a). For this report, we excluded participants with missing data, participants currently being treated with psychoactive medication, individuals with medical disorders that could impact brain function, and participants with poor image quality (see below). Eight-hundred thirty-one subjects met criteria and were included in the study (Figure 1). The average age of participants was 15.6 years (standard deviation (SD) = 3.4). Forty-two percent (n = 353) were male and 58% were female (n = 478). The institutional review boards of both the University of Pennsylvania and the Children's Hospital of Philadelphia approved all study procedures.

METHOD DETAILS

Cognitive assessment—Cognition was assessed using the University of Pennsylvania Computerized Neurocognitive Battery (CNB) (Gur et al., 2012). Accuracy of neurocognitive performance was measured across all tests included in the CNB, with raw measures of accuracy being normalized across the entire PNC. Executive function (EF) was summarized using a previously published factor analysis of the CNB (Moore et al., 2015). Each participant's *z*-score from this factor analysis was used to evaluate associations between executive function and CBF-ALFF coupling.

Image acquisition—PNC imaging was acquired at a single site with a 3T Siemens Tim Trio scanner with a 32-channel head coil (Erlangen, Germany), as previously described (Satterthwaite et al., 2014a). To minimize motion, prior to data acquisition, subjects' heads were stabilized in the head coil using one foam pad over each ear and a third over the top of the head.

High-resolution structural images were acquired to facilitate alignment of individual subject images into a common space. Structural images were acquired using a 3D-encoded magnetization-prepared, rapid-acquisition gradient-echo (MPRAGE) T1-weighted sequence (T_R = 1810 ms; T_E = 3.51 ms; FoV = 180 × 240 mm; matrix size = 192 × 256, number of slices = 160, slice thickness/gap = 1mm/0; resolution 0.9375 × 0.9375 × 1 mm).

Approximately 6 minutes of task-free functional data were acquired for each subject using a blood oxygen level-dependent (BOLD-weighted) 2D EPI sequence (T_R = 3000 ms; T_E = 32 ms; FoV = 192 × 192 mm; matrix size = 64 × 64; number of slices = 46; slice thickness/gap = 3mm/0; resolution 3 mm isotropic; 124 volumes). A fixation cross was displayed as images were acquired. Subjects were instructed to stay awake, keep their eyes

open, fixate on the displayed crosshair, and remain still. Brain perfusion was imaged with a 3D-encoded spin-echo pseudocontinuous arterial spin labeling (pCASL) sequence (T_R = 4000 ms; T_E = 15 ms; FoV = 220 × 220 mm; matrix size = 96 × 96; number of slices = 20; slice thickness/gap = 5/1mm; resolution 2.3 × 2.3 × 6 mm; 80 volumes).

Quality assurance—Quality assurance was performed separately for each modality. T1-weighted images were excluded for low quality images and/or low quality in FreeSurfer reconstruction (Fischl, 2012). Task-free BOLD scans were excluded if the mean framewise displacement was higher than 0.2 mm, or if there were more than 20 frames with motion exceeding 0.25 mm (Satterthwaite et al., 2014a). ASL images were excluded if they had excessive motion (mean framewise displacement >0.5 mm), low temporal signal-to-noise ratio (SNR <30), or an excessive number of voxels that reached ceiling intensity values (Kaczkurkin et al., 2016; Satterthwaite et al., 2014b).

Image processing—The structural images were processed using FreeSurfer (version 5.3) to allow for the projection of ALFF and CBF to the cortical surface (Fischl, 2012). Resting-state fMRI scans were processed using a top-performing preprocessing pipeline implemented using the eXtensible Connectivity Pipelines (XCP) (Ciric et al., 2018), which includes tools from FSL (Jenkinson et al., 2012; Smith et al., 2004) and AFNI (Cox, 1996). This pipeline included (1) correction for distortions induced by magnetic field inhomogeneity using FSL's FUGUE utility, (2) removal of the initial 4 volumes for resting-state fMRI, (3) realignment of all volumes to a selected reference volume using FSL's MCFLIRT, (4) interpolation of intensity outliers in each voxel's time series using AFNI's 3dDespike utility, (5) demeaning and removal of any linear or quadratic trends, and (6) co-registration of functional data to the high-resolution structural image using boundary-based registration. Images were denoised using a 36-parameter confound regression model. This model included the six framewise estimates of motion, the mean signal extracted from eroded white matter and cerebrospinal fluid compartments, the mean signal extracted from the entire brain, the derivatives of each of these nine parameters, and quadratic terms of each of the nine parameters and their derivatives. This method has previously been shown to appropriately identify motion-contaminated volumes in the BOLD time series and reduce their impact on further analysis (Ciric et al., 2017). Both the BOLD-weighted time series and the arti-factual model time series were then temporally filtered using a first-order Butterworth filter with a passband between 0.01 and 0.08 Hz to avoid mismatch in the temporal domain (Hallquist et al., 2013). The voxel-wise ALFF was computed as the sum over frequency bins in the low-frequency (0.01–0.08 Hertz) band of the power spectrum using a Fourier transform of the time-domain signal (Cordes et al., 2001).

CBF was quantified from control-label pairs in the following equation:

$$f = \frac{\Delta M \lambda R_{1a} \exp(\omega R_{1a})}{2 M_0 a} [1 - \exp(-\tau R_{1a})]^{-1},$$

where f is CBF, ΔM is the difference signal between the control and label acquisitions, R_{1a} is the longitudinal relaxation rate of blood, τ is the labeling time, ω is the postlabeling delay time, α is the labeling efficiency, λ is the blood/tissue water partition coefficient, and M_0

is approximated by the control image intensity (Wang et al., 2008). We set $\alpha = 0.85$, $\lambda = 0.9$ g/mL, $\tau = 1.6$ s, and $\omega = 1.2$ s. Participant-level CBF images were co-registered to the corresponding T1-weighted image using boundary-based registration with six degrees of freedom (Greve and Fischl, 2009). Given that T1 relaxation time differs according to age and sex (Biagi et al., 2007; Hales et al., 2014; Taki et al., 2011), the T1 relaxation parameter was modeled on an age- and sex-specific basis (Wu et al., 2010). This has been shown to enhance the accuracy and reliability of results in developmental samples (Jain et al., 2012; Satterthwaite et al., 2014b).

The CBF and ALFF maps for each individual were projected to the participant's anatomic surface and smoothed with a 6 mm full-width half-maximum (FWHM) kernel. The smoothed data were normalized to the *fsaverage5* template, which has 10,242 vertices on each hemisphere (18,715 vertices in total after removing the medial wall).

CBF-ALFF coupling—Coupling maps were generated at the cortical surface using methods as previously described in detail (Vandekar et al., 2016). For each vertex, a 15-mm FWHM neighborhood was defined and a locally weighted regression where ALFF was predicted by CBF was fit. This was repeated at all vertices within each subject, generating one CBF-ALFF coupling map where each vertex was represented by the coupling regression slope (Figure 2). A group mean coupling map was also generated by averaging the mean t-statistic of each individual's CBF-ALFF slope at a given vertex.

To minimize the possibility that our findings were driven by relationships in areas with poor SNR, we removed vertices with SNR<50 from our coupling analyses. Furthermore, we used spin-based permutation testing to confirm that there was no relationship between the mean CBF-ALFF coupling map and SNR in the retained locations (Alexander-Bloch et al., 2018).

QUANTIFICATION AND STATISTICAL ANALYSIS

We sought to evaluate how neurovascular coupling develops and relates to biological sex and executive function. CBF-ALFF coupling maps for each participant were used for statistical analyses. Generalized additive models (GAMs) were used to calculate linear and nonlinear age and sex effects at each vertex using the following model:

$$\text{Coupling}_{\text{vertex}} = \text{spline(age)} + \text{sex} + \text{CBF motion} + \text{ALFF motion} + \text{error}.$$

This approach allowed for flexible modeling of both linear and nonlinear effects. For significance testing, smooth terms were fitted as fixed degrees of freedom regression splines (k = 4). We also fit the model with an age-by-sex interaction; however, it was not significant and thus removed from the model. To assess the relationship between coupling and executive function accuracy, we fit a second model which included a linear executive accuracy term in addition to the above model's covariates (spline of age, sex, CBF and ALFF motion, and error). GAMs were estimated using the R package 'mgcv' in CRAN (Wood, 2021). All analyses controlled the False.

Discovery rate (FDR) at $Q < 0.05$. to estimate *the* variance in subject-level data explained by each of our regressors in our GAMs, we calculated partial correlation coefficients (r^2)—In addition to these analyses of effects at each vertex, we also evaluated the relationship between whole-brain coupling and age non-linearly. We first computed a single mean t-statistic per subject by averaging the t-statistics for the slope at each vertex that met FDR correction, and then used a GAM to estimate the relationship between each subject's mean coupling and age. To test for windows of significant change across the age range, we calculated the first derivative of the smooth function of age from the GAM model using finite differences, and then generated a simultaneous 95% confidence interval of the derivative using the R package 'gratia' (Larsen et al., 2020; Simpson and Singmann, 2021; Wood, 2021). Intervals of significant change were identified as areas where the simultaneous confidence interval of the derivative did not include zero.

Network enrichment analyses via spin testing—Given that patterns of neural activity differ across functional networks (Raut et al., 2020), we sought to characterize whether effects of interest tended to be located within specific functional brain networks (Buckner and Krienen, 2013; Thomas Yeo et al., 2011). To do this, we conducted network enrichment analyses. Specifically, we evaluated whether mean coupling and significant associations with variables of interest (age, sex, executive function) were preferentially located in one or more of the seven large-scale functional networks defined by Yeo et al. (Thomas Yeo et al., 2011). To account for the different size of each network and the spatial autocorrelation of brain maps, statistical testing used a conservative spin-based spatial permutation procedure (Alexander-Bloch et al., 2018). Briefly, statistical maps from association testing were projected onto a sphere, which was rotated 1,000 times per hemisphere to create a null distribution. For the mean coupling enrichment analysis, the test statistic was the mean t-value for each of the seven networks from Yeo et al. For the regression analyses, the test statistic was the proportion of vertices that survived FDR correction. Networks were considered to have significant enrichment if the test statistic in the observed data was in the top 5% of the null distribution derived from permuted data.

ACKNOWLEDGMENTS

This work was primarily supported by grants from the National Institute of Mental Health (NIMH): R01MH112847 to T.D.S. and R.T.S.; R01MH120482 and R01MH113550 to T.D.S.; R01 MH123550-01 to R.T.S.; R01MH107235 to R.C.G.; 2T32MH019112-29A1 to E.B.B.; T32MH014654 to B.L.L.; F31MH123063-01A1 to A.R.P.; R01MH120174, R01MH119185, and R56AG066656 to D.R.R.; DGE1845298 to V.J.S. The PNC was funded by RC2 grants MH089983 and MH089924 to R.E.G. from the NIMH. Additional support was provided by the AE Foundation, the Penn-CHOP Lifespan Brain Institute, the Penn Brain Science Center, and the Penn Center for Biomedical Image Computing and Analysis.

REFERENCES

Alexander-Bloch A, Shou H, Liu S, Satterthwaite TD, Glahn DC, Shinohara RT, Vandekar SN, and Raznahan A (2018). On testing for spatial correspondence between maps of human brain structure and function. Neuroimage 178, 540–551. 10.1016/j.neuroimage.2018.05.070. [PubMed: 29860082]

Arain M, Haque M, Johal L, Mathur P, Nel W, Rais A, Sandhu R, and Sharma S (2013). Maturation of the adolescent brain. Neuropsychiatr. Dis. Treat 9, 449–461. 10.2147/NDT.S39776. [PubMed: 23579318]

Armstead WM (2016). Cerebral blood flow autoregulation and dysautoregulation. Anesthesiol Clin. 34, 465–477. 10.1016/j.anclin.2016.04.002. [PubMed: 27521192]

Attwell D, and Laughlin SB (2001). An energy budget for signaling in the grey matter of the brain. J. Cereb. Blood Flow Metab 21, 1133–1145. 10.1097/00004647-200110000-00001. [PubMed: 11598490]

Ball G, Beare R, and Seal ML (2019). Charting shared developmental trajectories of cortical thickness and structural connectivity in childhood and adolescence. Hum. Brain Mapp 40, 4630–4644. 10.1002/hbm.24726. [PubMed: 31313446]

Baller EB, Kaczkurkin AN, Sotiras A, Adebimpe A, Bassett DS, Calkins ME, Chand G, Cui Z, Gur RE, Gur RC, et al. (2020). Neurocognitive and functional heterogeneity in depressed youth. Neuropsychopharmacology 46, 783–790. 10.1038/s41386-020-00871-w. [PubMed: 33007777]

Bassett DS, Bullmore E, Verchinski BA, Mattay VS, Weinberger DR, and Meyer-Lindenberg A (2008). Hierarchical organization of human cortical networks in health and schizophrenia. J. Neurosci 28, 9239–9248. 10.1523/JNEUROSCI.1929-08.2008. [PubMed: 18784304]

Baum GL, Cui Z, Roalf DR, Ciric R, Betzel RF, Larsen B, Cieslak M, Cook PA, Xia CH, Moore TM, et al. (2020). Development of structure–function coupling in human brain networks during youth. PNAS 117, 771–778. 10.1073/pnas.1912034117. [PubMed: 31874926]

Bazinet V, de Wael RV, Hagmann P, Bernhardt BC, and Misic B (2020). Multiscale communication in cortico-cortical networks. Preprint at bioRxiv. 10.1101/2020.10.02.323030.

Bercury KK, and Macklin WB (2015). Dynamics and mechanisms of CNS myelination. Dev. Cell 32, 447–458. 10.1016/j.devcel.2015.01.016. [PubMed: 25710531]

Berman KF, Schmidt PJ, Rubinow DR, Danaceau MA, Van Horn JD, Esposito G, Ostrem JL, and Weinberger DR (1997). Modulation of cognition-specific cortical activity by gonadal steroids: a positron-emission tomography study in women. Proc. Natl. Acad. Sci. U S A 94, 8836–8841. [PubMed: 9238064]

Beul SF, and Hilgetag CC (2019). Neuron density fundamentally relates to architecture and connectivity of the primate cerebral cortex. Neuroimage 189, 777–792. 10.1016/j.neuroimage.2019.01.010. [PubMed: 30677500]

Biagi L, Abbruzzese A, Bianchi MC, Alsop DC, Guerra AD, and Tosetti M (2007). Age dependence of cerebral perfusion assessed by magnetic resonance continuous arterial spin labeling. J. Magn. Reson. Imaging 25, 696–702. 10.1002/jmri.20839. [PubMed: 17279531]

Biswal B, Yetkin FZ, Haughton VM, and Hyde JS (1995). Functional connectivity in the motor cortex of resting human brain using echo-planar mri. Magn. Reson. Med 34, 537–541. 10.1002/mrm.1910340409. [PubMed: 8524021]

Blanco VM, Stern JE, and Filosa JA (2008). Tone-dependent vascular responses to astrocyte-derived signals. Am. J. Physiol. Heart Circ. Physiol 294, H2855–H2863. 10.1152/ajpheart.91451.2007. [PubMed: 18456724]

Bu X, Hu X, Zhang L, Li B, Zhou M, Lu L, Hu X, Li H, Yang Y, Tang W, et al. (2019). Investigating the predictive value of different resting-state functional MRI parameters in obsessive-compulsive disorder. Transl Psychiatry 9, 1–10. 10.1038/s41398-018-0362-9. [PubMed: 30664621]

Buckner RL, and Krienen FM (2013). The evolution of distributed association networks in the human brain. Trends Cogn. Sci 17, 648–665. 10.1016/j.tics.2013.09.017. [PubMed: 24210963]

Calkins ME, Merikangas KR, Moore TM, Burstein M, Behr MA, Satterthwaite TD, Ruparel K, Wolf DH, Roalf DR, Mentch FD, et al. (2015). The Philadelphia Neurodevelopmental Cohort: constructing a deep phenotyping collaborative. J. Child Psychol. Psychiatry 56, 1356–1369. [PubMed: 25858255]

Chung YS, Poppe A, Novotny S, Epperson CN, Kober H, Granger DA, Blumberg HP, Ochsner K, Gross JJ, Pearlson G, and Stevens MC (2019). A preliminary study of association between adolescent estradiol level and dorsolateral prefrontal cortex activity during emotion regulation. Psychoneuroendocrinology 109, 104398. 10.1016/j.psyneuen.2019.104398. [PubMed: 31394491]

Ciric R, Rosen AFG, Erus G, Cieslak M, Adebimpe A, Cook PA, Bassett DS, Davatzikos C, Wolf DH, and Satterthwaite TD (2018). Mitigating head motion artifact in functional connectivity MRI. Nat. Protoc 13, 2801–2826. 10.1038/s41596-018-0065-y. [PubMed: 30446748]

Ciric R, Wolf DH, Power JD, Roalf DR, Baum GL, Ruparel K, Shinohara RT, Elliott MA, Eickhoff SB, Davatzikos C, et al. (2017). Bench-marking of participant-level confound regression strategies for the control of motion artifact in studies of functional connectivity. Neuroimage 154, 174–187. [PubMed: 28302591]

Cordes D, Haughton VM, Arfanakis K, Carew JD, Turski PA, Moritz CH, Quigley MA, and Meyerand ME (2001). Frequencies contributing to functional connectivity in the cerebral cortex in "Resting-state" data. AJNR Am. J. Neuroradiol 22, 1326–1333. [PubMed: 11498421]

Cox RW (1996). AFNI: software for analysis and visualization of functional magnetic resonance neuroimages. Comput. Biomed. Res 29, 162–173. 10.1006/cbmr.1996.0014. [PubMed: 8812068]

Detre JA, and Alsop DC (1999). Perfusion magnetic resonance imaging with continuous arterial spin labeling: methods and clinical applications in the central nervous system. Eur. J. Radiol 30, 115–124. 10.1016/S0720-048X(99)00050-9. [PubMed: 10401592]

Dhamala E, Jamison KW, Sabuncu MR, and Kuceyeski A (2019). Sex classification using long-range temporal dependence of resting-state functional MRI time series. Preprint at bioRxiv. 10.1101/809954.

Dosenbach NUF, Fair DA, Miezin FM, Cohen AL, Wenger KK, Dosenbach RAT, Fox MD, Snyder AZ, Vincent JL, Raichle ME, et al. (2007). Distinct brain networks for adaptive and stable task control in humans. PNAS 104, 11073–11078. [PubMed: 17576922]

Elston GN, Oga T, and Fujita I (2009). Spinogenesis and pruning scales across functional hierarchies. J. Neurosci 29, 3271–3275. [PubMed: 19279264]

Fawcett JW, Oohashi T, and Pizzorusso T (2019). The roles of perineuronal nets and the perinodal extracellular matrix in neuronal function. Nat. Rev. Neurosci 20, 451–465. 10.1038/s41583-019-0196-3. [PubMed: 31263252]

Fischl B (2012). Freesurfer. Neuroimage 62, 774–781. 10.1016/j.neuroimage.2012.01.021. [PubMed: 22248573]

Fitzgerald KD, Liu Y, Stern ER, Welsh RC, Hanna GL, Monk CS, Luan Phan K, and Taylor SF (2013). Reduced error-related activation of dorsolateral prefrontal cortex across pediatric anxiety disorders. J. Am. Acad. Child Adolesc. Psychiatry 52, 1183–1191.e1. 10.1016/j.jaac.2013.09.002. [PubMed: 24157392]

Garrett DD, Lindenberger U, Hoge RD, and Gauthier CJ (2017). Age differences in brain signal variability are robust to multiple vascular controls. Scientific Rep. 7, 10149. 10.1038/s41598-017-09752-7.

Giedd JN, Blumenthal J, Jeffries NO, Castellanos FX, Liu H, Zijdenbos A, Paus T, Evans AC, and Rapoport JL (1999). Brain development during childhood and adolescence: a longitudinal MRI study. Nat. Neurosci 2, 861. [PubMed: 10491603]

Gilbert DL, Huddleston DA, Wu SW, Pedapati EV, Horn PS, Hirabayashi K, Crocetti D, Wassermann EM, and Mostofsky SH (2019). Motor cortex inhibition and modulation in children with ADHD. Neurology 93, e599–e610. 10.1212/WNL.0000000000007899. [PubMed: 31315973]

Girouard H, and Iadecola C (2006a). Neurovascular coupling in the normal brain and in hypertension, stroke, and Alzheimer disease. J. Appl. Physiol 100, 328–335. 10.1152/japplphysiol.00966.2005. [PubMed: 16357086]

Girouard H, and Iadecola C (2006b). Neurovascular coupling in the normal brain and in hypertension, stroke, and Alzheimer disease. J. Appl. Physiol 100, 328–335. 10.1152/japplphysiol.00966.2005. [PubMed: 16357086]

Greve DN, and Fischl B (2009). Accurate and robust brain image alignment using boundary-based registration. Neuroimage 48, 63–72. [PubMed: 19573611]

Gündling P, Haneder J, and Gaab MR (1985). Correlation between CBF and pCO2, pO2, pH, hemoglobin, blood pressure, age, and sex. In Cerebral Blood Flow and Metabolism Measurement, Hartmann A and Hoyer S, eds. (Springer), pp. 51–55. 10.1007/978-3-642-70054-5_6.

Gur RC, Butler ER, Moore TM, Rosen AFG, Ruparel K, Satterthwaite TD, Roalf DR, Gennatas ED, Bilker WB, Shinohara RT, et al. (2021). Structural and functional brain parameters related to cognitive performance across development: replication and extension of the parieto-frontal integration theory in a single sample. Cereb. Cortex 31, 1444–1463. 10.1093/cercor/bhaa282. [PubMed: 33119049]

Gur RC, Richard J, Calkins ME, Chiavacci R, Hansen JA, Bilker WB, Loughead J, Connolly JJ, Qiu H, Mentch FD, et al. (2012). Age group and sex differences in performance on a computerized neurocognitive battery in children age 8–21. Neuropsychology 26, 251–265. 10.1037/a0026712. [PubMed: 22251308]

Hales PW, Kawadler JM, Aylett SE, Kirkham FJ, and Clark CA (2014). Arterial spin labeling characterization of cerebral perfusion during normal maturation from late childhood into adulthood: normal 'reference range' values and their use in clinical studies. J. Cereb. Blood Flow Metab 34, 776–784. 10.1038/jcbfm.2014.17. [PubMed: 24496173]

Hallquist MN, Hwang K, and Luna B (2013). The nuisance of nuisance regression: spectral misspecification in a common approach to resting-state fMRI preprocessing reintroduces noise and obscures functional connectivity. NeuroImage 82, 208–225. 10.1016/j.neuroimage.2013.05.116. [PubMed: 23747457]

Hu B, Yan L-F, Sun Q, Yu Y, Zhang J, Dai Y-J, Yang Y, Hu Y-C, Nan H-Y, Zhang X, et al. (2019). Disturbed neurovascular coupling in type 2 diabetes mellitus patients: evidence from a comprehensive fMRI analysis. Neuroimage Clin. 22, 101802. 10.1016/j.nicl.2019.101802. [PubMed: 30991623]

Jacobs B, Schall M, Prather M, Kapler E, Driscoll L, Baca S, Jacobs J, Ford K, Wainwright M, and Treml M (2001). Regional dendritic and spine variation in human cerebral cortex: a quantitative golgi study. Cereb. Cortex 11, 558–571. 10.1093/cercor/11.6.558. [PubMed: 11375917]

Jain V, Duda J, Avants B, Giannetta M, Xie SX, Roberts T, Detre JA, Hurt H, Wehrli FW, and Wang DJJ (2012). Longitudinal reproducibility and accuracy of pseudo-continuous arterial spin-labeled perfusion MR imaging in typically developing children. Radiology 263, 527–536. 10.1148/radiol.12111509. [PubMed: 22517961]

Janfaza M, Sherman TI, Larmore KA, Brown-Dawson J, and Klein KO (2006). Estradiol levels and secretory dynamics in normal girls and boys as determined by an ultrasensitive bioassay: a 10 year experience. J. Pediatr. Endocrinol. Metab 19, 901–909. 10.1515/jpem.2006.19.7.901. [PubMed: 16995570]

Jenkinson M, Beckmann CF, Behrens TEJ, Woolrich MW, and Smith SM (2012). FSL. NeuroImage, 20 YEARS OF fMRI 62. Neuroimage. 62, 782–790. 10.1016/j.neuroimage.2011.09.015. [PubMed: 21979382]

Jin M, Wang L, Wang H, Han X, Diao Z, Guo W, Yang Z, Ding H, Wang Z, Zhang P, et al. (2020). Disturbed neurovascular coupling in hemo-dialysis patients. PeerJ 8, e8989. 10.7717/peerj.8989. [PubMed: 32328355]

Jung J, Cloutman LL, Binney RJ, and Lambon Ralph MA (2017). The structural connectivity of higher order association cortices reflects human functional brain networks. Cortex 97, 221–239. 10.1016/j.cortex.2016.08.011. [PubMed: 27692846]

Kaczkurkin AN, Moore TM, Ruparel K, Ciric R, Calkins ME, Shinohara RT, Elliott MA, Hopson R, Roalf DR, Vandekar SN, et al. (2016). Elevated amygdala perfusion mediates developmental sex differences in trait anxiety. Biol. Psychiatry 80, 775–785. 10.1016/j.biopsych.2016.04.021. [PubMed: 27395327]

Kaiser RH, Andrews-Hanna JR, Wager TD, and Pizzagalli DA (2015). Large-scale network dysfunction in Major Depressive Disorder: meta-analysis of resting-state functional connectivity. JAMA Psychiatry 72, 603–611. 10.1001/jamapsychiatry.2015.0071. [PubMed: 25785575]

Kety S (1957). The general metabolism of the brain *in vivo*. In Metabolism of the Nervous System (Pergamon), pp. 221–237.

Kim KJ, and Filosa JA (2012). Advanced *in vitro* approach to study neurovascular coupling mechanisms in the brain microcirculation. J. Physiol 590, 1757–1770. 10.1113/jphysiol.2011.222778. [PubMed: 22310311]

Krause DN, Duckles SP, and Gonzales RJ (2011). Local estrogenic/androgenic balance in the cerebral vasculature. Acta Physiol. (Oxf) 203, 181–186. 10.1111/j.1748-1716.2011.02323.x. [PubMed: 21535417]

Larsen B, Bourque J, Moore TM, Adebimpe A, Calkins ME, Elliott MA, Gur RC, Gur RE, Moberg PJ, Roalf DR, et al. (2020). Longitudinal development of brain iron is linked to cognition in youth. J. Neurosci 40, 1810–1818. 10.1523/JNEUROSCI.2434-19.2020. [PubMed: 31988059]

Li Z, Zhu Y, Childress AR, Detre JA, and Wang Z (2012). Relations between BOLD fMRI-derived resting brain activity and cerebral blood flow. PLoS One 7, e44556. 10.1371/journal.pone.0044556. [PubMed: 23028560]

Liang X, Zou Q, He Y, and Yang Y (2013). Coupling of functional connectivity and regional cerebral blood flow reveals a physiological basis for network hubs of the human brain. PNAS 110, 1929–1934. 10.1073/pnas.1214900110. [PubMed: 23319644]

Liu F, Duan Y, Peterson BS, Asllani I, Zelaya F, Lythgoe D, and Kangarlu A (2018). Resting state cerebral blood flow with arterial spin labeling MRI in developing human brains. Eur. J. Paediatric Neurol 22, 642–651. 10.1016/j.ejpn.2018.03.003.

Liu Y, Zhu X, Feinberg D, Guenther M, Gregori J, Weiner MW, and Schuff N (2012). Arterial spin labeling MRI study of age and gender effects on brain perfusion hemodynamics. Magn. Reson. Med 68, 912–922. 10.1002/mrm.23286. [PubMed: 22139957]

Livesey D, Keen J, Rouse J, and White F (2006). The relationship between measures of executive function, motor performance and externalising behaviour in 5- and 6-year-old children. Hum. Mov Sci 25, 50–64. 10.1016/j.humov.2005.10.008. [PubMed: 16442172]

Lourenço CF, Ledo A, Caetano M, Barbosa RM, and Laranjinha J (2018). Age-dependent impairment of neurovascular and neurometabolic coupling in the Hippocampus. Front Physiol. 9, 913. 10.3389/fphys.2018.00913. [PubMed: 30065657]

Miller DJ, Duka T, Stimpson CD, Schapiro SJ, Baze WB, McArthur MJ, Fobbs AJ, Sousa AMM, Šestan N, Wildman DE, et al. (2012). Prolonged myelination in human neocortical evolution. Proc. Natl. Acad. Sci. U S A 109, 16480–16485. 10.1073/pnas.1117943109. [PubMed: 23012402]

Miyake A, Friedman NP, Emerson MJ, Witzki AH, Howerter A, and Wager TD (2000). The unity and diversity of executive functions and their contributions to complex “Frontal Lobe” tasks: a latent variable analysis. Cogn. Psychol 41, 49–100. 10.1006/cogp.1999.0734. [PubMed: 10945922]

Moore TM, Reise SP, Gur RE, Hakonarson H, and Gur RC (2015). Psychometric properties of the Penn computerized neurocognitive battery. Neuropsychology 29, 235. [PubMed: 25180981]

Mulligan SJ, and MacVicar BA (2004). Calcium transients in astrocyte end-feet cause cerebrovascular constrictions. Nature 431, 195–199. 10.1038/nature02827. [PubMed: 15356633]

Nomi JS, Bolt TS, Ezie CEC, Uddin LQ, and Heller AS (2017). Moment-to-Moment BOLD signal variability reflects regional changes in neural flexibility across the lifespan. J. Neurosci 37, 5539–5548. 10.1523/JNEUROSCI.3408-16.2017. [PubMed: 28473644]

Paquola C, Bethlehem RA, Seidlitz J, Wagstyl K, Romero-Garcia R, Whitaker KJ, Vos de Wael R, Williams GB, Consortium NSPN, Vértes PE, et al. (2019). Shifts in myeloarchitecture characterise adolescent development of cortical gradients. eLife 8, e50482. 10.7554/eLife.50482. [PubMed: 31724948]

Passow S, Specht K, Adamsen TC, Biermann M, Brekke N, Craven AR, Ersland L, Grüner R, Kleven-Madsen N, Kvernenes O-H, et al. (2015). Default-mode network functional connectivity is closely related to metabolic activity. Hum. Brain Mapp 36, 2027–2038. 10.1002/hbm.22753. [PubMed: 25644693]

Phillips AA, Chan FH, Zheng MMZ, Krassioukov AV, and Ainslie PN (2016). Neurovascular coupling in humans: physiology, methodological advances and clinical implications. J. Cereb. Blood Flow Metab 36, 647–664. 10.1177/0271678X15617954. [PubMed: 26661243]

Presa JL, Saravia F, Bagi Z, and Filosa JA (2020). Vasculo-neuronal coupling and neurovascular coupling at the neurovascular unit: impact of hypertension. Front. Physiol 11, 584135. 10.3389/fphys.2020.584135. [PubMed: 33101063]

Proisy M, Bruneau B, Rozel C, Tréguier C, Chouklati K, Riffaud L, Darnault P, and Ferré J-C (2016). Arterial spin labeling in clinical pediatric imaging. Diagn. Interv. Imaging 97, 151–158. 10.1016/j.diii.2015.09.001. [PubMed: 26456912]

Qiu M, Scheinost D, Ramani R, and Constable RT (2017). Multi-modal analysis of functional connectivity and cerebral blood flow reveals shared and unique effects of propofol in large-scale brain networks. Neuroimage 148, 130–140. 10.1016/j.neuroimage.2016.12.080. [PubMed: 28069540]

Raut RV, Snyder AZ, and Raichle ME (2020). Hierarchical dynamics as a macroscopic organizing principle of the human brain. PNAS 117, 20890–20897. 10.1073/pnas.2003383117. [PubMed: 32817467]

Raz N, Rodrigue KM, Kennedy KM, and Acker JD (2007). Vascular health and longitudinal changes in brain and cognition in middle-aged and older adults. Neuropsychology 21, 149–157. 10.1037/0894-4105.21.2.149. [PubMed: 17402815]

Reding KM, Wei S-M, Martinez PE, Nguyen T-V, Gregory MD, Kippenhan JS, Kohn PD, Soldin SJ, Nieman LK, Yanovski JA, et al. (2021). The NIMH intramural longitudinal study of the endocrine and neurobiological events accompanying puberty: protocol and rationale for. Neuroimage 234, 117970. 10.1016/j.neuroimage.2021.117970. [PubMed: 33771694]

Satterthwaite TD, Connolly JJ, Ruparel K, Calkins ME, Jackson C, Elliott MA, Roalf DR, Hopson R, Prabhakaran K, Behr M, et al. (2016). The Philadelphia Neurodevelopmental Cohort: a publicly available resource for the study of normal and abnormal brain development in youth. Neuroimage 124, 1115–1119. [PubMed: 25840117]

Satterthwaite TD, Elliott MA, Ruparel K, Loughead J, Prabhakaran K, Calkins ME, Hopson R, Jackson C, Keefe J, Riley M, et al. (2014a). Neuroimaging of the Philadelphia neurodevelopmental Cohort. Neuroimage 86, 544–553. [PubMed: 23921101]

Satterthwaite TD, Shinohara RT, Wolf DH, Hopson RD, Elliott MA, Vandekar SN, Ruparel K, Calkins ME, Roalf DR, Gennatas ED, et al. (2014b). Impact of puberty on the evolution of cerebral perfusion during adolescence. Proc. Natl. Acad. Sci 111, 8643–8648. [PubMed: 24912164]

Satterthwaite TD, Wolf DH, Erus G, Ruparel K, Elliott MA, Gennatas ED, Hopson R, Jackson C, Prabhakaran K, Bilker WB, et al. (2013). Functional maturation of the executive system during adolescence. J. Neurosci 33, 16249–16261. [PubMed: 24107956]

Schulte T, Hong J-Y, Sullivan EV, Pfefferbaum A, Baker FC, Chu W, Prouty D, Kwon D, Meloy MJ, Brumback T, et al. (2020). Effects of age, sex, and puberty on neural efficiency of cognitive and motor control in adolescents. Brain Imaging Behav. 14, 1089–1107. 10.1007/s11682-019-00075-x. [PubMed: 30903550]

Seney ML, and Sibille E (2014). Sex differences in mood disorders: perspectives from humans and rodent models. Biol. Sex Differ 5, 17. 10.1186/s13293-014-0017-3. [PubMed: 25520774]

Sepulcre J, Liu H, Talukdar T, Martincorena I, Yeo BTT, and Buckner RL (2010). The organization of local and distant functional connectivity in the human brain. PLoS Comput. Biol 6, e1000808. 10.1371/journal.pcbi.1000808. [PubMed: 20548945]

Shanmugan S, Wolf DH, Calkins ME, Moore TM, Ruparel K, Hopson RD, Vandekar SN, Roalf DR, Elliott MA, Jackson C, et al. (2016). Common and dissociable mechanisms of executive system dysfunction across psychiatric disorders in youth. Am. J. Psychiatry 173, 517–526. 10.1176/appi.ajp.2015.15060725. [PubMed: 26806874]

Shokri-Kojori E, Tomasi D, Alipanahi B, Wiers CE, Wang G-J, and Volkow ND (2019). Correspondence between cerebral glucose metabolism and BOLD reveals relative power and cost in human brain. Nat. Commun 10, 690. 10.1038/s41467-019-08546-x. [PubMed: 30741935]

Silverman A, and Petersen NH (2022). Physiology, Cerebral Autoregulation. [Updated 2022 Feb 16]. In StatPearls [Internet] (Treasure Island (FL): StatPearls Publishing), Available from: https://www.ncbi.nlm.nih.gov/books/NBK553183/.

Simpson GL, and Singmann H (2021). Gratia: Graceful 'ggplot'-Based Graphics and Other Functions for GAMs Fitted Using "Mgcv" (GitHub).

Smith SM, Jenkinson M, Woolrich MW, Beckmann CF, Behrens TEJ, Johansen-Berg H, Bannister PR, De Luca M, Drobnjak I, Flitney DE, et al. (2004). Advances in functional and structural MR image analysis and implementation as FSL. Neuroimage 23 (Suppl 1), S208–S219. 10.1016/j.neuroimage.2004.07.051. [PubMed: 15501092]

Sokoloff L (1996). Cerebral metabolism and visualization of cerebral activity. In Comprehensive Human Physiology: From Cellular Mechanisms to Integration, Greger R and Windhorst U, eds. (Springer), pp. 579–602. 10.1007/978-3-642-60946-6_30.

Sorond FA, Schnyer DM, Serrador JM, Milberg WP, and Lipsitz LA (2008). Cerebral blood flow regulation during cognitive tasks: effects of healthy aging. Cortex 44, 179–184. 10.1016/j.cortex.2006.01.003. [PubMed: 18387547]

Spedden ME, Malling ASB, Andersen KK, and Jensen BR (2017). Association between gross-motor and executive function depends on age and motor task complexity. Dev. Neuropsychol 42, 495–506. 10.1080/87565641.2017.1399129. [PubMed: 29161178]

Stadelmann C, Timmler S, Barrantes-Freer A, and Simons M (2019). Myelin in the central nervous system: structure, function, and pathology. Physiol. Rev 99, 1381–1431. 10.1152/physrev.00031.2018. [PubMed: 31066630]

Stöckel T, and Hughes CML (2016). The relation between measures of cognitive and motor functioning in 5- to 6-year-old children. Psychol. Res 80, 543–554. 10.1007/s00426-015-0662-0. [PubMed: 25820330]

Stuhr C, Hughes CML, and Stöckel T (2020). The role of executive functions for motor performance in preschool children as compared to young adults. Front. Psychol 11, 1552. [PubMed: 32774313]

Suminaite D, Lyons DA, and Livesey MR (2019). Myelinated axon physiology and regulation of neural circuit function. Glia 67, 2050–2062. 10.1002/glia.23665. [PubMed: 31233642]

Sydnor VJ, Larsen B, Bassett DS, Alexander-Bloch A, Fair DA, Liston C, Mackey AP, Milham MP, Pines A, Roalf DR, et al. (2021). Neurodevelopment of the association cortices: patterns, mechanisms, and implications for psychopathology. Neuron 109, 2820–2846. 10.1016/j.neuron.2021.06.016. [PubMed: 34270921]

Sylvester CM, Corbetta M, Raichle ME, Rodebaugh T, Schlaggar BL, Sheline YI, Zorumski CF, and Lenze EJ (2012). Functional network dysfunction in anxiety and anxiety disorders. Trends Neurosci. 35, 527–535. 10.1016/j.tins.2012.04.012. [PubMed: 22658924]

Takano T, Tian G-F, Peng W, Lou N, Libionka W, Han X, and Nedergaard M (2006). Astrocyte-mediated control of cerebral blood flow. Nat. Neurosci 9, 260–267. 10.1038/nn1623. [PubMed: 16388306]

Taki Y, Hashizume H, Sassa Y, Takeuchi H, Wu K, Asano M, Asano K, Fukuda H, and Kawashima R (2011). Gender differences in partial-volume corrected brain perfusion using brain MRI in healthy children. Neuroimage 58, 709–715. 10.1016/j.neuroimage.2011.07.020. [PubMed: 21782958]

Tamnes CK, Herting MM, Goddings A-L, Meuwese R, Blakemore S-J, Dahl RE, Güroğlu B, Raznahan A, Sowell ER, Crone EA, and Mills KL (2017). Development of the cerebral cortex across adolescence: a multisample study of inter-related longitudinal changes in cortical volume, surface area, and thickness. J. Neurosci 37, 3402–3412. 10.1523/JNEUROSCI.3302-16.2017. [PubMed: 28242797]

Thomas Yeo BT, Krienen FM, Sepulcre J, Sabuncu MR, Lashkari D, Hollinshead M, Roffman JL, Smoller JW, Zöllei L, Polimeni JR, et al. (2011). The organization of the human cerebral cortex estimated by intrinsic functional connectivity. J. Neurophysiol 106, 1125–1165. 10.1152/jn.00338.2011. [PubMed: 21653723]

Tong Y, Hocke LM, Lindsey KP, Erdoğan SB, Vitaliano G, Caine CE, and deB. Frederick B (2016). Systemic low-frequency oscillations in BOLD signal vary with tissue type. Front Neurosci. 10, 313. 10.3389/fnins.2016.00313. [PubMed: 27445680]

Toth P, Tarantini S, Csiszar A, and Ungvari Z (2017). Functional vascular contributions to cognitive impairment and dementia: mechanisms and consequences of cerebral autoregulatory dysfunction, endothelial impairment, and neurovascular uncoupling in aging. Am. J. Physiology-Heart Circulatory Physiol 312, H1–H20. 10.1152/ajpheart.00581.2016.

van der Fels IMJ, Te Wierike SCM, Hartman E, Elferink-Gemser MT, Smith J, and Visscher C (2015). The relationship between motor skills and cognitive skills in 4–16 year old typically developing children: a systematic review. J. Sci. Med. Sport 18, 697–703. 10.1016/j.jsams.2014.09.007. [PubMed: 25311901]

Vandekar SN, Shinohara RT, Raznahan A, Hopson RD, Roalf DR, Ruparel K, Gur RC, Gur RE, and Satterthwaite TD (2016). Subject-level measurement of local cortical coupling. NeuroImage 133, 88–97. 10.1016/j.neuroimage.2016.03.002. [PubMed: 26956908]

Vandekar SN, Shinohara RT, Raznahan A, Roalf DR, Ross M, DeLeo N, Ruparel K, Verma R, Wolf DH, Gur RC, et al. (2015). Topologically dissociable patterns of development of the human cerebral cortex. J. Neurosci 35, 599–609. 10.1523/JNEUROSCI.3628-14.2015. [PubMed: 25589754]

Váša F, Seidlitz J, Romero-Garcia R, Whitaker KJ, Rosenthal G, Vértes PE, Shinn M, Alexander-Bloch A, Fonagy P, Dolan RJ, et al. (2018). Adolescent tuning of association cortex in human structural brain networks. Cereb. Cortex 28, 281–294. 10.1093/cercor/bhx249. [PubMed: 29088339]

Vázquez-Rodríguez B, Suárez LE, Markello RD, Shafiei G, Paquola C, Hagmann P, van den Heuvel MP, Bernhardt BC, Spreng RN, and Misic B (2019). Gradients of structure–function tethering across neocortex. PNAS 116, 21219–21227. [PubMed: 31570622]

Wade M, Zeanah CH, Fox NA, and Nelson CA (2020). Global deficits in executive functioning are transdiagnostic mediators between severe childhood neglect and psychopathology in adolescence. Psychol. Med 50, 1687–1694. 10.1017/S0033291719001764. [PubMed: 31391139]

Wang J, Licht DJ, Jahng G-H, Liu C-S, Rubin JT, Haselgrove J, Zimmerman RA, and Detre JA (2003). Pediatric perfusion imaging using pulsed arterial spin labeling. J. Magn. Reson. Imaging 18, 404–413. 10.1002/jmri.10372. [PubMed: 14508776]

Wang Z, Aguirre GK, Rao H, Wang J, Fernández-Seara MA, Childress AR, and Detre JA (2008). Empirical optimization of ASL data analysis using an ASL data processing toolbox: ASLtbx. Magn. Reson. Imaging 26, 261–269. 10.1016/j.mri.2007.07.003. [PubMed: 17826940]

Williams LR, and Leggett RW (1989). Reference values for resting blood flow to organs of man. Clin. Phys. Physiol. Meas 10, 187–217. 10.1088/0143-0815/10/3/001. [PubMed: 2697487]

Wood S (2021). Mgcv: Mixed GAM Computation Vehicle with Automatic Smoothness Estimation (CRAN).

Wood S, Goude Y, and Shaw S (2015). Generalized additive models for large datasets. J. R. Stat. Soc. Ser. C Appl. Stat 64, 139–155. 10.1111/rssc.12068.

Wu W-C, Jain V, Li C, Giannetta M, Hurt H, Wehrli FW, and Wang DJJ (2010). In vivo venous blood T1 measurement using inversion recovery true-FISP in children and adults. Magn. Reson. Med 64, 1140–1147. 10.1002/mrm.22484. [PubMed: 20564586]

Xing C-Y, Tarumi T, Liu J, Zhang Y, Turner M, Riley J, Tinajero CD, Yuan L-J, and Zhang R (2017). Distribution of cardiac output to the brain across the adult lifespan. J. Cereb. Blood Flow Metab 37, 2848–2856. 10.1177/0271678X16676826. [PubMed: 27789785]

Ye FQ, Berman KF, Ellmore T, Esposito G, van Horn JD, Yang Y, Duyn J, Smith AM, Frank JA, Weinberger DR, and McLaughlin AC (2000). H(2)(15)O PET validation of steady-state arterial spin tagging cerebral blood flow measurements in humans. Magn. Reson. Med 44, 450–456. 10.1002/1522-2594(200009)44:3<450::aid-mrm16>3.0.co;2-0. [PubMed: 10975898]

Yu-Feng Z, Yong H, Chao-Zhe Z, Qing-Jiu C, Man-Qiu S, Meng L, Li-Xia T, Tian-Zi J, and Yu-Feng W (2007). Altered baseline brain activity in children with ADHD revealed by resting-state functional MRI. Brain Develop. 29, 83–91. 10.1016/j.braindev.2006.07.002.

Yurgelun-Todd D (2007). Emotional and cognitive changes during adolescence. Curr. Opin. Neurobiol 17, 251–257. 10.1016/j.conb.2007.03.009. [PubMed: 17383865]

Zheng W, Cui B, Han Y, Song H, Li K, He Y, and Wang Z (2019). Disrupted regional cerebral blood flow, functional activity and connectivity in alzheimer's disease: a combined ASL perfusion and resting state fMRI study. Front. Neurosci 13, 738. 10.3389/fnins.2019.00738. [PubMed: 31396033]

Zou Q-H, Zhu C-Z, Yang Y, Zuo X-N, Long X-Y, Cao Q-J, Wang Y-F, and Zang Y-F (2008). An improved approach to detection of amplitude of low-frequency fluctuation (ALFF) for resting-state fMRI: fractional ALFF. J. Neurosci. Methods 172, 137–141. 10.1016/j.jneumeth.2008.04.012. [PubMed: 18501969]

Highlights

- Cerebral blood flow and amplitude of low-frequency fluctuations are coupled in youth
- CBF-ALFF coupling declines during adolescence in the dorsal attention network
- Sex differences in CBF-ALFF coupling are prominent in the frontoparietal network
- Coupling patterns are associated with individual differences in executive function

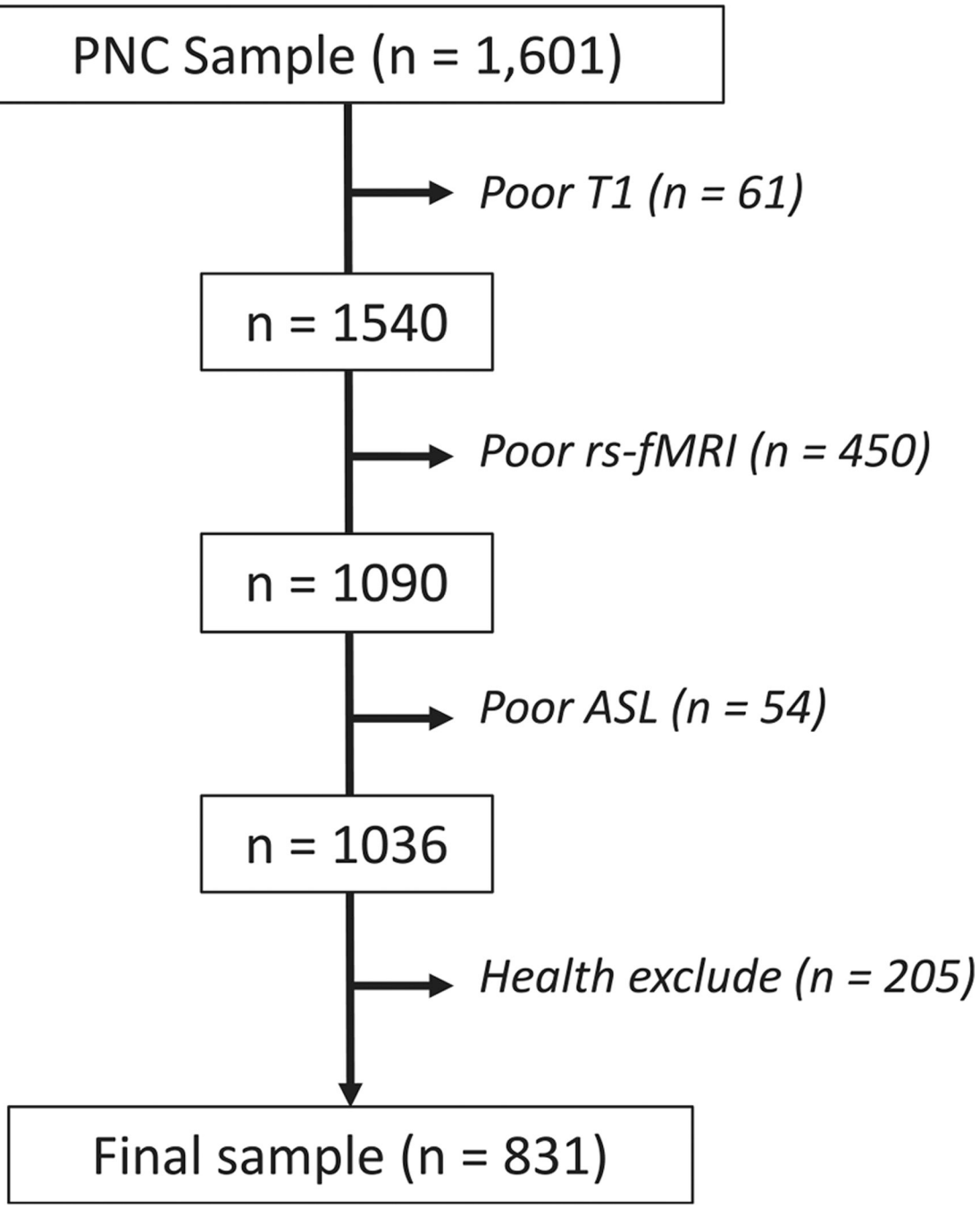

Figure 1. Sample construction

A total of 1,601 participants had neuroimaging scans acquired as part of the PNC, and 831 were included in the study after excluding those who failed rigorous quality assessment for poor T1 quality (n = 61), resting-state fMRI quality (n = 450), ASL quality (n = 54), and medical and psychiatric comorbidities (n = 205).

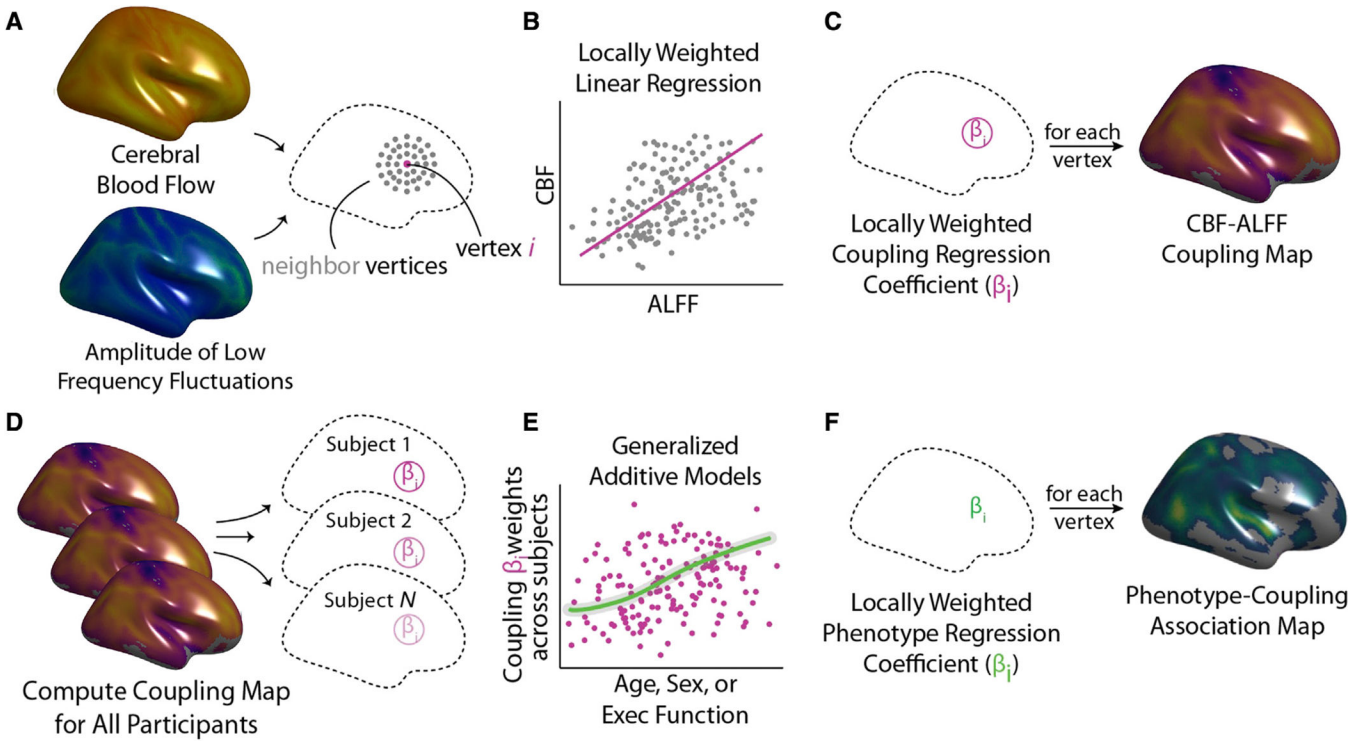

Figure 2. Analysis of CBF-ALFF coupling

CBF-ALFF coupling analysis involves both calculation of within-subject coupling and across-subject comparisons to assess individual differences.

(A) For each subject, a neighborhood for each vertex was identified.

(B) Locally weighted regressions of ALFF onto CBF were calculated.

(C) Locally weighted regressions were repeated at each vertex, resulting in a participant-level coupling map.

(D and E) After subject-level coupling maps were calculated, statistical analyses relating covariates of interest (e.g., age, sex, and executive function) to participant-level coupling maps were calculated using generalized additive models (GAMs).

(F) GAMs were fit at each vertex, yielding a group-level statistical map describing individual differences.

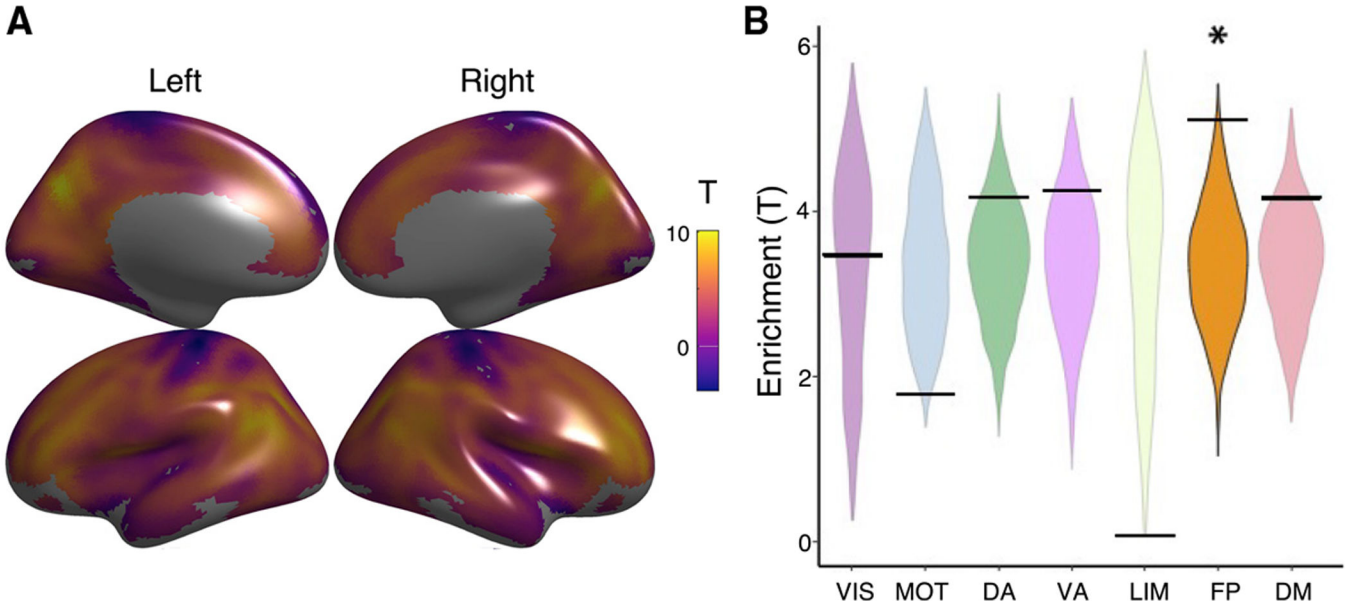

Figure 3. Mean CBF-ALFF coupling

(A) CBF-ALFF coupling is robust throughout the brain, with maximal coupling in the medial and lateral prefrontal cortex, parietal cortex, posterior cingulate. and precuneus. (B) We used a spin-based spatial permutation test that accounted for spatial autocorrelation to evaluate enrichment of CBF-ALFF coupling in canonical functional networks. This revealed enrichment in the frontoparietal network ($p = 0.005$). The asterisk represents statistical significance ($p < 0.05$). The black bars represent the observed values, whereas the violin plots reflect the null distributions.

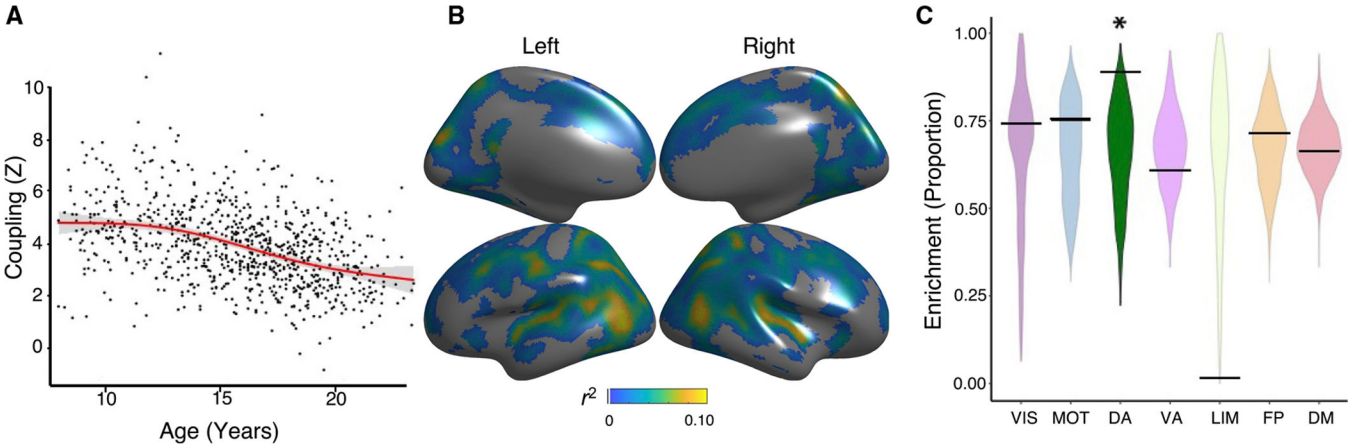

Figure 4. CBF-ALFF coupling evolves with age

Linear and nonlinear age effects of CBF-ALFF were flexibly modeled within a generalized additive model at each vertex, while controlling for sex and in-scanner motion; multiple comparisons were controlled using the false discovery rate ($Q < 0.05$).

(A) Mean cortical CBF-ALFF coupling declines with age in a nonlinear fashion ($F_{3,828} = 60.0$, $p < 0.0001$). Data points represent the mean CBF-ALFF coupling (Z) for each subject (n = 831) across all vertices that met statistical correction ($p_{fdr} < 0.05$).

(B) Vertex-level CBF-ALFF declines were prominent in the posterior temporal cortex, parietal cortex, and dorsolateral prefrontal cortex. Partial correlation coefficients (r^2) are displayed to show the strength of effects.

(C) Spin testing revealed enrichment of age effects within the dorsal attention network ($p = 0.027$). The asterisk represents statistical significance. Black bars represent the observed values, whereas the violin plots reflect the null distributions.

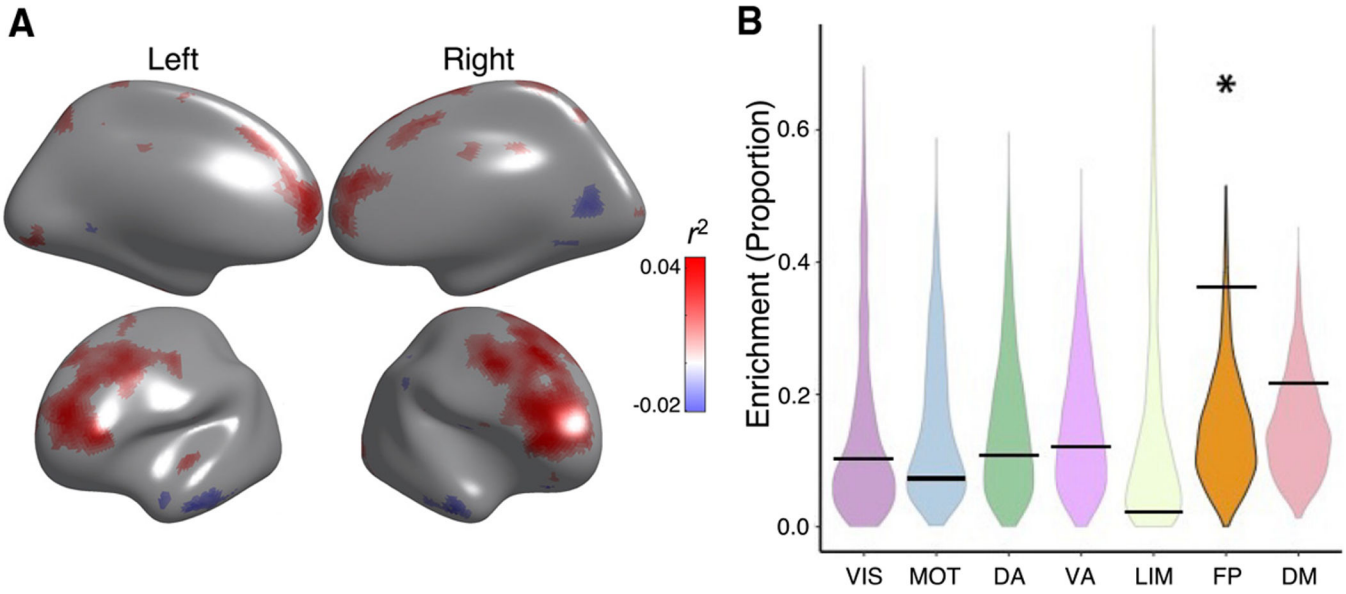

Figure 5. Sex differences in CBF-ALFF coupling

(A) CBF-ALFF coupling is higher in females than males in the bilateral dorsolateral prefrontal cortex, medial frontal cortex, anterior cingulate cortex, and precuneus. CBF-ALFF coupling differences between females and males were modeled using generalized additive models, while adjusting for both linear and nonlinear age effects as well as in-scanner motion; multiple comparisons were controlled using the false discovery rate ($Q < 0.05$). Partial correlation coefficients (r^2) are displayed to show strength of effects. For visualization purposes, regions where females had higher coupling have a positive r^2 and are shown in red, whereas regions where males had higher coupling have a negative r^2 and are shown in blue.

(B) Spin testing revealed significant enrichment of sex differences within the frontoparietal network ($p = 0.032$). The asterisk represents statistical significance. Black bars represent the observed values, whereas the violin plots reflect the null distributions.

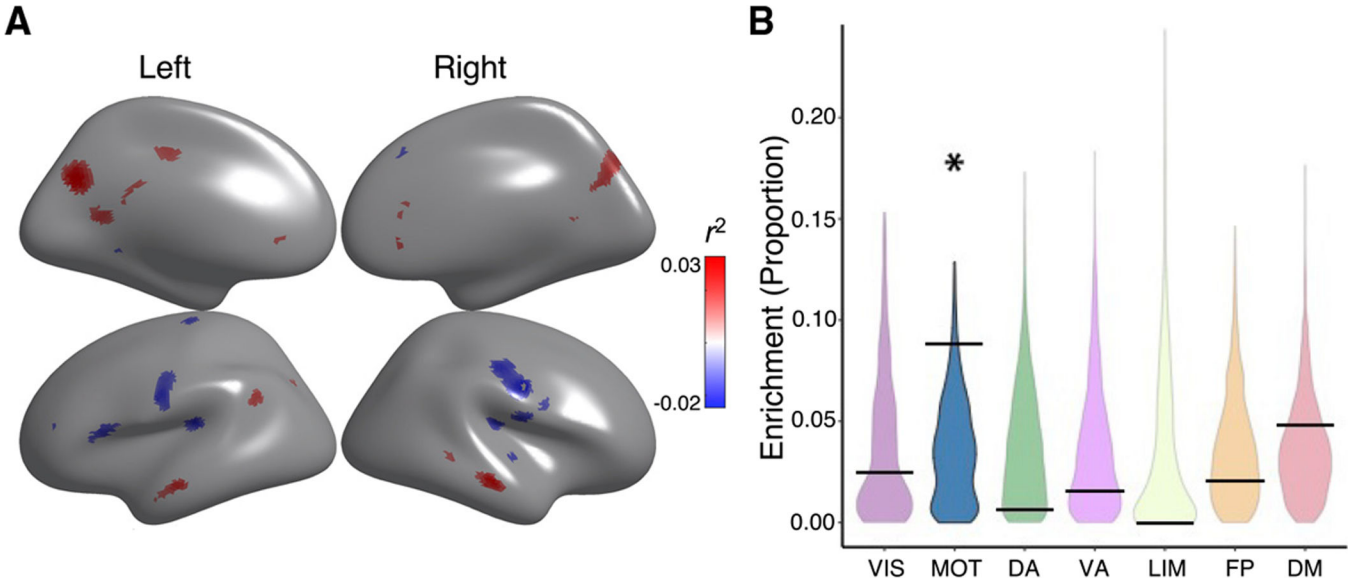

Figure 6. CBF-ALFF coupling is related to executive function

(A) The relationship of CBF-ALFF coupling to executive function showed regional variation, with both positive and negative associations. Generalized additive models were used to calculate the relationship between CBF-ALFF coupling and executive function while controlling for linear and nonlinear age effects, sex effects, and in-scanner motion; multiple comparisons were accounted for using the false discovery rate ($Q < 0.05$). Higher coupling in parts of the default mode were associated with better executive functioning, while higher coupling in parts of the somatomotor network were associated with reduced executive functioning. Partial correlation coefficients (r^2 values) are displayed to show strength of effects. For visualization purposes, regions with positive associations have a positive r^2 and are shown in red, whereas regions with negative associations have a negative r^2 and are shown in blue.

(B) Spin testing revealed that associations between executive function and coupling were significantly enriched in the motor network ($p = 0.040$). The asterisk represents statistical significance ($p < 0.05$). Black bars represent the observed values, whereas the violin plots reflect the null distributions.

KEY RESOURCES TABLE

REAGENT or RESOURCE	SOURCE	IDENTIFIER
Deposited data		
Raw and preprocessed ASL perfusion, BOLD resting-state fMRI, clinical and cognitive data	Philadelphia Neurodevelopmental Cohort	https://www.ncbi.nlm.nih.gov/projects/gap/cgi-bin/study.cgi?study_id=phs000607.v3.p2
Software and algorithms		
R 3.6.3	R Foundation	https://cran.r-project.org/bin/macosx/
Matlab 2020b	Mathworks	https://www.mathworks.com/products/get-matlab.html?s_tid=gn_getml
Coupling and network enrichment analyses	This paper	https://doi.org/10.5281/zenodo.6320541
Other		
Resource website for Intermodal Coupling workflow	This paper	https://pennlinc.github.io/IntermodalCoupling/